An improved soot formation model for 3D diesel engine simulations

Boulanger, Joan; Liu, Fengshan; Neill, W. Stuart; Smallwood, Gregory J.

Publisher's version / Version de l'éditeur:
https://doi.org/10.1115/1.2718234
Journal of Engineering for Gas Turbines and Power, 129, 3, pp. 877-884, 2007-07

An Improved Soot Formation Model for 3D Diesel Engine Simulations

Joan Boulanger[1]
e-mail: joan.boulanger@nrc-cnrc.gc.ca

Fengshan Liu

W. Stuart Neill

Gregory J. Smallwood

Institute for Chemical Process and Environmental Technology,
1200 Montréal Building M-9,
Ottawa, ON, K1A0R6, Canada

Soot formation phenomenon is far from being fully understood today and models available for simulation of soot in practical combustion devices remain of relatively limited success, despite significant progresses made over the last decade. The extremely high demand of computing time of detailed soot models make them unrealistic for simulation of multidimensional, transient, and turbulent diesel engine combustion. Hence, most of the investigations conducted in real configuration such as multidimensional diesel engines simulation utilize coarse modeling, the advantages of which are an easy implementation and low computational cost. In this study, a phenomenological three-equation soot model was developed for modeling soot formation in diesel engine combustion based on considerations of acceptable computational demand and a qualitative description of the main features of the physics of soot formation. The model was developed based on that of Tesner et al. and was implemented into the commercial STAR-CD™ CFD package. Application of this model was demonstrated in the modeling of soot formation in a single-cylinder research version of Caterpillar 3400 series diesel engine with exhaust gas recirculation (EGR). Numerical results show that the new soot formulation overcomes most of the drawbacks in the existing soot models dedicated to this kind of engineering task and demonstrates a robust and consistent behavior with experimental observation. Compared to the existing soot models for engine combustion modeling, some distinct features of the new soot model include: no soot is formed at low temperature, minimal model parameter adjustment for application to different fuels, and there is no need to prescribe the soot particle size. At the end of expansion, soot is predicted to exist in two separate regions in the cylinder: in the near wall region and in the center part of the cylinder. The existence of soot in the near wall region is a result of reduced soot oxidation rate through heat loss. They are the source of the biggest primary particles released at the end of the combustion process. The center part of the cylinder is populated by smaller soot particles, which are created since the early stages of the combustion process but also subject to intense oxidation. The qualitative effect of EGR is to increase the size of soot particles as well as their number density. This is linked to the lower in-cylinder temperature and a reduced amount of air. [DOI: 10.1115/1.2718234]

Keywords: soot modeling, diesel engine, emission, particle, automotive engineering

Introduction

The merits of diesel engines, compared to other internal combustion engines, are lower fuel consumption, and unburned hydrocarbons, due to the overall lean combustion (equivalence ratio of the order of 0.5), and a better energy release efficiency due to a controlled nonhomogeneous combustion (diffusion flame) at high pressures. Diesel engine is therefore an attractive option to reduce CO_2 emissions from automobiles and counter greenhouse gas effects [1]. On the other hand, because of the existence of rich high temperature zones leading to fuel pyrolysis, a diesel engine is very likely to produce particulates emission in the exhaust gas. Given the intensive use of diesel engines and the detrimental effects of soot particulates on environment and health [2], more stringent emissions standards have been imposed [3], which challenge the viability of diesel engines.

Soot formation phenomenon is far from being fully understood despite the significant progress in fundamental understanding made in the last two decades. Simple engineering correlations and simplified soot formation models available for simulation of soot in practical combustion devices remain of relatively limited success. In the early 1970s, Khan and Greeves [4] presented the first model for the soot production from diesel engines. The most complete models describing soot dynamics formation use chemical kinetics-like approach, as in Refs. [5–8]. However, because of the numerous Arrhenius terms appearing in these models, it is questionable to use this type of modeling for simulation of multidimensional, transient, and turbulent diesel engine combustion. Beside this "kinetic approach," "empirical approaches" are also widely used, particularly for soot formation prediction in industrial configurations. The majority of the phenomenological approaches belong to the one-step fuel based models [4,9,10]. Indisputably, most of the modern numerical studies on multidimensional diesel engine computation with prediction of soot emission [1,11–20] have been made with the help of those empirical models, which consist of only one Arrhenius term in the soot formation step with two empirical constants: a moderately high activation temperature and a preexponential constant. The advantages of these empirical soot models are easy implementation and low computational costs but with the drawbacks of an often poor representation of the physical and chemical processes.

[1]Present address: Gas Turbine Laboratory–Institute for Aerospace Research, National Research Council of Canada, Building M-10 Room 104, 1200 Montréal Road, K1A 0R6 Ottawa, ON, Canada.

Contributed by the Internal Combustion Engine Division of ASME for publication in the JOURNAL OF ENGINEERING FOR GAS TURBINES AND POWER. Manuscript received January 23, 2006; final manuscript received December 13, 2006. Review conducted by Jim Cowart. Paper presented at the 2005 Fall Conference of the ASME Internal Combustion Engine Division (ICEF2005), September 11–14, 2005, Ottawa, ON, Canada.

These models thus in general suffer a narrow range of applicability around the conditions under which they were developed.

It is well established that soot formation is divided into two major steps: *inception* and *growth*, both following the pyrolysis of fuel, a decomposition and incomplete combustion of hydrocarbons (HC). Each of them may be further divided into two substeps. First, inception is related to the formation of soot precursors, whose nature is not clearly defined yet, but generally believed to be sufficiently large polycyclic aromatic hydrocarbons (PAHs) [7], produced as intermediate products directly from fuel pyrolysis and then conversion through polymerization into particulate nuclei when a sufficient mass is reached. This is also the initial stage that a physical surface appears. Second, soot particulate surface growth proceeds through the addition of carbon atoms by heterogeneous reaction at the surface of the particulate with the pyrolysis products and coagulation. Eventually, when they get older, primary particles assemble in fractal clusters. Clearly, actual soot formation models dedicated to industrial configuration simulations are unable to capture all aspects of the phenomena. However, given the new emission standards, it becomes important to better characterize the soot formation process in order to improve the design of an engine by incorporating efficiently the key knowledge on soot dynamics to meet the current and forthcoming regulations on particulate emission.

It is intended in this paper to develop a computationally efficient phenomenological soot model within the context of diesel engine combustion. The following two criteria were sought during the development of the present model: (i) capture of the main physical processes of soot formation, and (ii) without significant increase in computing time or the complexity of the formalism. The soot model developed in this study was incorporated into the STAR-CD™ package. Its capability was demonstrated in particulate emission prediction from a single-cylinder research version of the Caterpillar™ 3400 series diesel engine with exhaust gas recirculation (EGR).

Development of a Three-Equation Model

The present model is derived from the Tesner et al. model [21]. This model has the advantage of embedding the representative generic steps related to soot particle formation in a system of two Semenov equations. The interest is in complementing this model by a soot particle surface growth process, which can help establishing an explicit link between fuel concentration and soot mass growth. This alleviates the requirement for an ad hoc prescribed diameter of the primary soot particles in the original model of Tesner et al. (given a soot particle number density distribution in the cylinder volume, prescription of the size results in a major nuisance of the soot mass distribution without any consideration for the physics of soot formation/combustion dynamics). The other expected benefits are a reduced tuning process—for most of the parameters may be identified with the help of fundamental data—and a good computation efficiency since the equations are kept relatively simple and not too nonlinear, compared to the existing models. It is thus hoped that most of the interesting features of soot formation dynamics can be predicted at a low computational cost, convenient for engineering applications. Given the relatively poor knowledge on cluster formation, the model is only able to predict the primary particle size and history but not soot aggregates.

Regulatory agencies are more and more interested in knowing the emitted particle size from industrial furnaces or engines [2,3], rather than the soot mass only, for the following two reasons. First, the smaller particles are actually more deleterious to human health and environment [22,23]. Second, although modern diesel engines have lower particulate emissions, they often emit particles that are smaller in size but larger in number density, as a result of the technical solutions adopted to decrease the overall soot mass production. Emission control systems for particulate matter are not always efficient in retaining all soot particles, depending on their respective size ($<$50 nm) [24]. Diesel particle filters rely on two distinct technologies: *strain filtration* or *deep bed filtration*. In case of strain filtration, the consequences of small particles are obvious as they escape through the perforated medium acting as a filter and are freely released to the atmosphere. However, even deep bed filtration technology efficiency is damaged for small particles have less chance of collision with the filter when they go through the SiC fibers. Attempts of predicting the primary particle size characteristic of the emission represent a challenge for numerical predictive tools dedicated to diesel engine design and are the first step before considering the cluster formation modeling, which form the effective entities to be trapped.

Several models simulate the surface growth rate of soot particles through interactions between the surface density of soot primary particles and the surrounding fuel vapor [5,25] (or its break-down products [6,8]). The usual form of this growth process may be written as

$$K_G N[\text{Fuel}]A_s \tag{1}$$

which describes the heterogeneous reaction of the surrounding fuel molecules at the surface A_s of the soot primary particles. Here NA_s is the volumetric density of available soot particle surface area, associated with a locally monodispersed primary particle distribution. In Eq. (1), [Fuel] is the molar concentration of the hydrocarbon fuel and K_G is physically observed as a time-decaying constant modeling the saturation and stabilization of the active sites on soot particle surface during its growth. Such a time function is not convenient to implement and the models used in Refs. [5,6,8,25,26] make use of the undesirable Arrhenius term. Another somewhat crude way of handling the aging effect of soot particles is to consider it as inversely proportional to the area of soot particles, i.e., $K_G = K_{G,\text{incep}}/A_s$ ($K_{G,\text{incep}}$ represents the constant associated with inception soot particles—it is different from K_G as it includes A_s), thus canceling the surface dependence of the surface growth rate given in Eq. (1). In Ref. [26], the surface dependence was reduced to its square-root for a similar reason. In the present study, the assumption that K_G is inversely proportional to A_s is made in favor of simplicity, as the goal is to use a minimum set of rate equations that can describe the most important soot phenomena. Constant $K_{G,\text{incep}}$ is derived from the kinetic theory describing the collision frequency between Brownian particles (here the original hydrocarbon molecules) and the inception primary soot particles, assumed of spherical shape with a size and an inertia much larger than the hydrocarbon molecules. It was also assumed that the collision between a hydrocarbon molecule and an inception primary soot particle yields the release of all carbon atoms in the original fuel hydrocarbon molecule [5] and this assumption is also made in the present formulation. Hence, $K_{G,\text{incep}}$ is written as

$$K_{G,\text{incep}} = \sqrt{\frac{8RT}{\pi \bar{M}_F}} \frac{\pi D_0^2}{4} \bar{M}_c m \tag{2}$$

where $\bar{M}_F$ and $\bar{M}_c$ are the molar weights of fuel and carbon, respectively, D_0 is the inception diameter of soot particles. m represents the number of carbon atoms in the hydrocarbon molecule.

As mentioned earlier, soot particle growth is due to heterogeneous reaction involving growth species which are obtained from fuel breakdown. Directly linking soot growth to fuel concentration is obviously an approximation. Given that, to first order, fuel and HC-growth species coexist in space, it is assumed that soot growth is satisfactorily mimicked by reactions with primary fuel molecules, as has already been done for Fenimore reburn NO mechanism [27].

Furthermore, inception of soot particle from radicals also contributes to an initial amount of carbon matter and can be evaluated by $C_a a n$ with $C_a = \rho_s (\pi D_0^3)/6$. The equation for particle formation in Ref. [21] can thus be split into the following two equations:

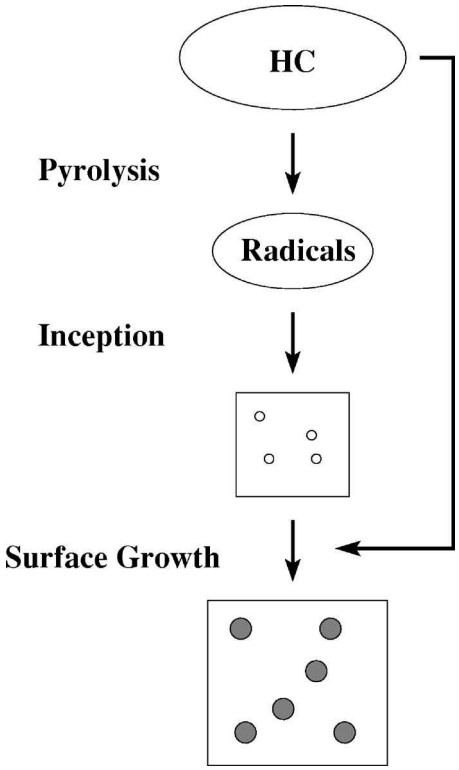

Fig. 1 Flow chart of the baseline soot model. HC is considered as the active specie at each step of the soot formation process for sake of simplicity and efficiency.

$$\frac{dN}{dt} = an - bNn \tag{3}$$

$$\frac{d(\rho y_s)}{dt} = K_{G,\text{incep}} N[\text{Fuel}] + C_a an - NA_s S_{\text{ox}} \tag{4}$$

that respectively describe the production rate of soot particle number density and soot mass. After taking into account the coagulation that reduces the soot particle number density, as suggested in Ref. [6], Eq. (3) takes the following form:

$$\frac{dN}{dt} = an - bNn - K_c\sqrt{T}\left(\frac{\rho y_s}{\rho_s}\right)^{1/6} N^{11/6} \tag{5}$$

with K_c being the coagulation coefficient.

The radical formation equation from Ref. [21] is retained here:

$$\frac{dn}{dt} = a_0 N_F \exp\left(-\frac{T_{a_{n_o}}}{T}\right) + Fn - g_0 Nn - S'_{\text{ox}} \tag{6}$$

Equations (4)–(6) constitute the three-equation soot model formulated in the present study. Figure 1 illustrates the physical and chemical processes leading to soot particles assumed in the formulation of the present soot model. First, as exhibited through the first term of Eq. (6), pyrolysis leads to the formation of radicals from fuel molecule cleavage. Those unstable radicals may increase in number through chain branching (second term) and may be destroyed when landing on soot particles (the last term). This is the original Semenov equation developed by Tesner et al. for the radicals [21]. As exhibited by the first term of Eq. (5) and the second term of Eq. (4), the presence of radicals leads to the assembling of nascent solid particles (diameter about 1 nm). Today's school of thinking interprets this with the help of PAH polymerization process. Once soot particles are formed, their growth is controlled by surface reaction and coalescence, the first and last terms of Eqs. (4) and (5), respectively. In the following, the reader will find a brief description of each term and the value assigned.

S_{ox} in Eq. (4) is the sum of the contribution of the following soot oxidation models. The oxidation by O_2 is given by the Nagle-Strickland-Constable [28] model (S_{NSC}). Soot oxidation by OH and O attacks are taken into account according to the Fenimore and Jones mechanism [29] (S_{FJ}) and the relation found in Ref. [30] (S_{BDEM}), respectively. Thus, we have

$$S_{\text{ox}} = S_{\text{NSC}} + S_{\text{FJ}} + S_{\text{BDEM}} \tag{7}$$

with

$$S_{\text{NSC}} = 1.2 \times 10^2 \times \left\{\frac{k_A P_{O_2}\chi}{1 + k_z P_{O_2}} + k_B P_{O_2}(1-\chi)\right\} \tag{8}$$

$$S_{\text{FJ}} = 1.27 \times 10^3 \Gamma_{\text{OH}} P_{\text{OH}} T^{-1/2} \tag{9}$$

$$S_{\text{BDEM}} = 665.5 \Gamma_{\text{O}} P_{\text{O}} T^{-1/2} \tag{10}$$

Symbols in Eqs (8)–(10) are specific constants of the models whose clear definition is detailed in the respective references. P_i is the partial pressure of specie "i." The collision efficiencies Γ_i are: $\Gamma_{\text{O}}=0.5$ and $\Gamma_{\text{OH}}=0.42\tanh(2664/T-2.8)+1)$.

Oxidation is included in the model with an assumption that it does not directly affect the soot particle number density N. However, a soot primary particle is considered as destroyed when its diameter falls below the inception diameter D_o, mimicking implosion of the smallest primary particles due to the volume oxidation [31]. The concentrations of O and OH radicals are estimated based on partial-equilibrium relations [32].

Given the poor knowledge on the nature of the generic radicals, the oxidation of the latter is treated using the Magnussen and Hjertager model [33] modified as in [17], and is based only on O_2,

$$S'_{\text{ox}} = An\frac{\varepsilon}{\kappa}\min\left(1, \frac{y_{O_2}}{y_s \upsilon_s + y_F \upsilon_F}\right)(1 - e^{-T/1800}) \tag{11}$$

A is the constant of the model. κ/ε is the characteristic turbulence time. y_{O_2} and y_F are the di-oxygen and fuel mass fraction, respectively. ν_s and ν_F are the stoichiometric oxygen requirements to burn 1 kg of soot and fuel, respectively. Radicals, soot, and fuel are present in this oxidation rate for radicals are they are all in competition to access oxygen.

The parameters of the present soot model are summarized in the following (in SI units):

- $T_{a_{n_o}} = 21{,}000$ K. This activation temperature is correlated to the energy bond break [21] and is consistent with the oxidative pyrolysis [31]. It is expected to be fuel-dependent, in relation with the degree of saturation of the hydrocarbon molecule. The discussion in Ref. [26] for hydrocarbon mixture (p. 291) has been followed here.
- $a = 10^5$ was suggested in Ref. [21], based on the characteristic time of primary particles assembling from radicals.
- $F = 100$, $g_0 = 10^{-15}$, $b = 8 \times 10^{-14}$ were taken from Tesner et al. [21] as a result of experimental-based inverse analysis for a radical chemistry modeled using Semenov equations. It should be noted that F vanishes when the radical production rate becomes small.
- Constant a_0 is usually related to the vibration frequency of the bond to be broken. Quantum mechanics builds a bridge between this frequency and the peak in the IR spectrum for simple molecules. Obviously, this theoretical approach is subject to large uncertainty for larger hydrocarbon molecules. Due to the lack of better information, a_0 is arbitrarily set at 2.3×10^{-3} Hz in this study. It should be mentioned that a_0 is the *only* parameter which needs to be arbitrarily adjusted. It has been actually found that prediction trends

are relatively smooth with respect to a_o, helpful to a fast tuning process.
- $\rho_s = 1900$ kg/m^3 is retained for soot density.
- $D_0 = 1$ nm is the diameter of the inception soot particle.

Soot and radicals are considered here as trace species and do not influence flow properties. The turbulent Schmidt number for soot transport is assumed to be 15, since the primary particles inertia is much larger than gaseous molecules. Turbulent transport is assumed to dominate all other modes.

Numerical Methods

The three-equation soot model was implemented into the STAR-CD™ CFD code. Since this CFD package has been widely used in engine modeling community, only a brief summary of some features is given in the following.

STAR-CD™ solves the compressible, turbulent, three-dimensional transient conservation equations for reacting multi-component gas mixtures with the flow dynamics of an evaporating liquid spray treated as Lagrangian statistical polydispersed parcels on finite-volume grids. Throughout this study, the original model's constants documented in Ref. [34] were used, unless otherwise stated.

The injection process includes the modeling of the flow in the nozzle hole and atomization. The atomization model was that given by Huh [34,35]. The injector pressure is virtually set at 190 MPa. However, the velocity profile versus time is the effective quantity specified in the simulation. It is extrapolated, given the requirement of the prescribed fuel consumption, from the experimental curve provided in Ref. [17] where it is seen that the profile has a nominal exit velocity of 580 m/s. This latter value yields a nozzle discharge coefficient of about 0.83, which is consistent with the most up-to-date real devices.

The spray is modeled by using the Reitz and Diwakar model [36] and has demonstrated strong consistency with experiments on jet penetration at diesel-like conditions [37]. Perfect rebound is assumed when impinging the cylinder walls [1].

The fuel is approximately represented by dodecane for thermodynamic properties (density, viscosity, etc.) and by *n*-heptane for the chemical properties, since diesel combustion models are usually calibrated for that specie. The built-in data are used [34]. Nevertheless, the saturation pressure is enhanced in order to reach the correct range of peak temperature and ignition delay, which is justified in light of the complex nature of real diesel fuels, i.e., lighter components evaporate earlier and participate to the first stages of combustion [14].

The initial mixture at the beginning of the simulation (Intake Valve Closure, 147° BTDC) corresponds to ambient air at intake conditions ($T=307$ K, $P=235$ kPa). It should be noted that the residual gas in the cylinder was not taken into account in the present simulation.

The compressible RNG turbulence model [38,34] is used as it has been shown that this model is well suited to account for turbulence dynamics in an engine cylinder [12,14]. Standard wall functions [34,39,40] are applied to momentum and heat transfer at wall boundaries. No crevice flow model is used.

The Shell multistep kinetics model is applied for auto-ignition. A "laminar-turbulent" characteristic time combustion model is activated to model the turbulent combustion after ignition.

Results and Discussions

The engine numerically simulated in this study is a single-cylinder version of Caterpillar™ 3400-series (3406) heavy-duty diesel engine. The engine has four valves, a displacement of 2.44 L, electronically controlled fuel injection, and produces 74.6 kW at 1800 rpm. Further details of the engine configuration are summarized in Table 1. This engine has been well characterized in experimental and computational studies [11–18,41].

Table 1 Geometric and physical parameters of the Caterpillar 3400 series diesel engine used in the numerical simulation

Bore	137.2	mm
Stroke	165.1	mm
Connecting rod length	263	mm
Displacement	2.44	L/cyl
compression ratio	15.1	
Piston crown	Mexican hat	
Squish height	4.221	mm
Engine speed	1740	rpm
Intake pressure	235	kPa
Intake temperature	307	K
Intake valve close timing	147	deg BTDC
Swirl ratio	Nominal	
Fuel injected	3.06×10^{-5}	kg
Injection pressure	190	MPa
Nozzle diameter	0.259	mm
Spray angle from head	27.5°	
Injector protrusion	3.2	mm

Experimental measurement of particulate emissions from this engine with and without EGR were carried out by Neill and Chippior [42]. The numerical calculations were conducted under similar conditions to the experiments.

The soot model developed in this study was validated in the calculations of soot emissions from the above-described research engine against experimental data. During the course of this numerical study, the engine was not fully equipped and crucial parameters to assess a model in detail, such as cylinder pressure, heat release, injection shape were missing. The AVL test case number seven thus appeared as the easiest one to set-up through a generic approach including: top-hat injection profile, no residual gas, and generic cylinder wall temperature. We are thus primarily interested in generating new information on pollutant formation. Details of the combustion chamber geometry are provided in Fig. 2. Due to the cyclic nature of the configuration around the cylinder axis, an unstructured mesh of 60° angle sector with a moving piston and containing a single nozzle located on the bisecting plane is simulated.

Figure 3 displays the history of the total in-cylinder soot mass (m_{total}), total soot particle number (N_{total}), and the characteristic soot primary particle diameter calculated from $\rho_s \pi \overline{D^3}/6 \times N_{\text{total}} = m_{\text{total}}$. The open circles are the experimental soot emission data from Ref. [42]. The soot emission data in the case of no EGR were used to adjust the value of a_0, which is the only parameter that is arbitrarily "tuned" and is expected to be fuel dependent. The one-equation Hiroyasu soot model [10], which has been widely used in diesel engine simulation [1,11–20], was also employed in the present calculations using the constants given in Ref. [17]. Although both the Hiroyasu and the present soot models are capable of predicting the correct trend of the effect of cooled EGR on soot emission, the present model offers insight into the effect of EGR on the soot particle number and size that otherwise cannot be gained in the Hiroyasu model. This is obtained by incorporating the inception from radicals as well as the heterogeneous reaction at the surface of the soot particle in a logical sequence with respect to physical phenomena. For instance, surface reactions clearly allow predicting an increase in the soot diameter [Fig. 3(*c*)], in case of EGR. It is noted that the existence of soot particles at TDC in this case is simply due to the re-injection of the soot-containing exhaust gas (without filter) into the intake. Surface reactions are a competition between surface growth, the first term in Eq. (4), and surface oxidation. With EGR, fuel is available for a longer period of time in the cylinder, which favors surface growth [as well as a stronger creation of particles, on Fig. 3(*b*)] and the temperature is lower, weakening surface oxidation. Furthermore, the incorporation of a step corresponding to the induction radicals involves a delay in soot formation [early time in Fig. 3(*a*)], which is consistent with experiment but is badly represented by the one-step model. This is explained by the low

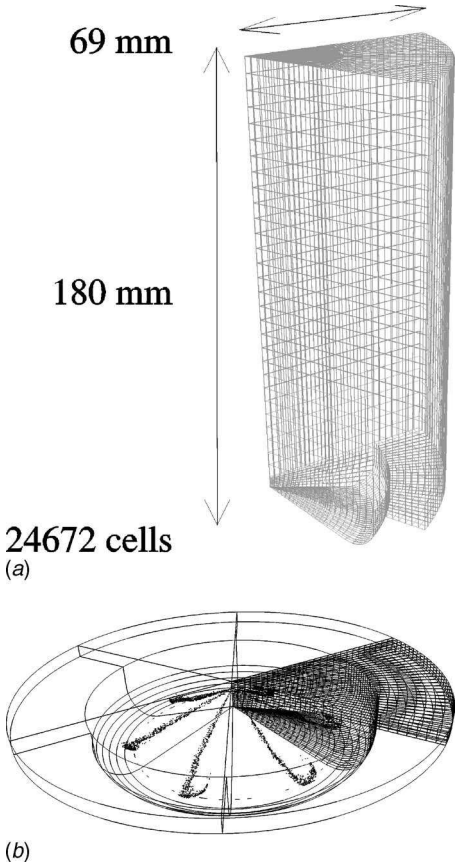

Fig. 2 CFD mesh of the cylinder geometry. Top panel: Full mesh sector (the sector picture has been stretched to show details on the layered part of the mesh subject to connectivity change and squeeze). Bottom panel: Full cylinder near TDC with spray impingement on the bowl.

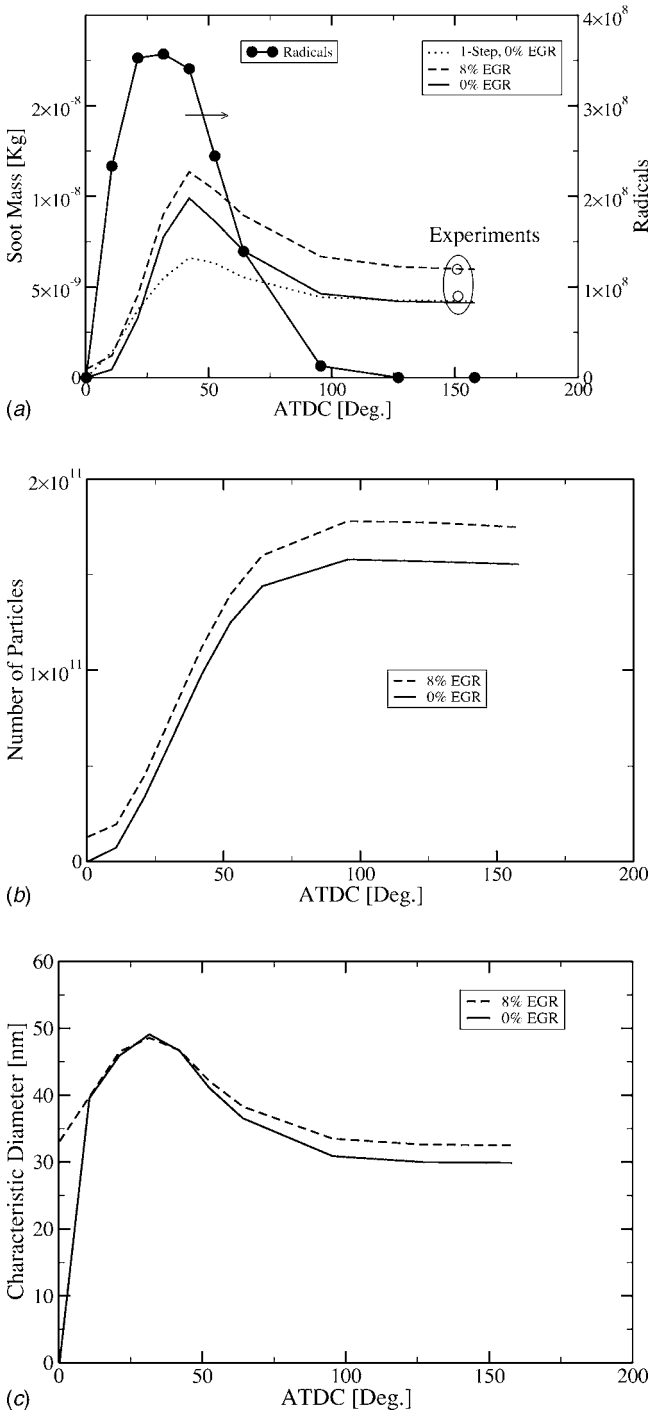

Fig. 3 History of the soot formation. (*a*) Soot mass. (*b*) Primary particle number. (*c*) Characteristic diameter. Line: present model. Dots: One-step model. Dashed line: Present model with 8% EGR. Line-circle: Induction radicals. Open circle: Experiment.

temperature dependence in the one-step model. The effect of this low temperature dependence may appear of secondary importance regarding the discrepancies induced in the overall soot production, as seen in Fig. 3(*a*). Nevertheless, the underlying consequence is the creation of soot mass in areas of the cylinder where it is physically prevented because the temperature was too low for pyrolysis/inception. Previous studies have demonstrated the importance of soot creation dynamics within the volume [8,43,44]. For instance, in Fig. 4, the soot contour in the median plan of the jet at the end of the injection is given for both models. It is seen that the one-step model predicts that soot is formed very early and close to the injector, a bias already pointed out in Ref. [45].

Coagulation is supposed to be weak, as predicted by the present model, Fig. 3(*b*). It has been suspected for two to three decades that the Brownian theory is insufficient to predict coagulation (and also agglomeration) in a highly turbulent in-cylinder flow [46,47]. However, only few very empirical approaches are currently available.

Figure 5 shows the predicted distribution of the primary particle size at the exhaust. This distribution is estimated on a cell by cell basis so that the characteristic diameter D_i of the particles contained in the cell i is given by

$$D_i = \left(\frac{6\rho y_{s_i}}{\pi \rho_s N_i} \right)^{1/3} \tag{13}$$

The weight associated with this diameter is proportional to the number of particles predicted within the cell.

Several observations are to be made. (i) The distribution of primary particle diameter lies in the acknowledged range for the diesel soot primary particle diameter, i.e., 10–50 nm. (ii) The overall diameter is increased through EGR, consistent with previous results. (iii) The distribution grossly presents two peaks. These two peaks may be explained by the existence of two soot primary particle populations inside the cylinder. These two populations are depicted in Fig. 5(*b*), where it is seen that soot with diameters below 20 nm (grossly, the left side of the distribution) are concentrated in the center of the cylinder and in the bowl while particles with a diameter larger than 40 nm are seen close to

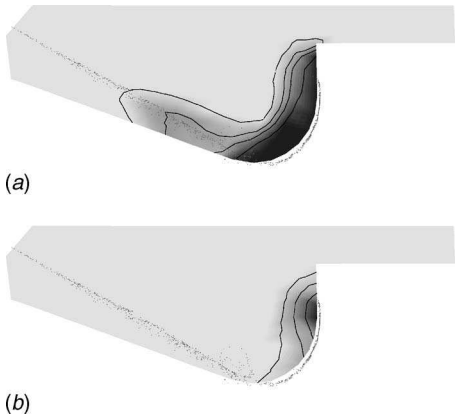

Fig. 4 Soot mass fraction distribution in the median plane of the fuel jet at the end of the injection. (*a*) One-step model. (*b*) Three-equation model.

the wall, Fig. 5(*a*). Population in the bowl and along the axis is represented by numerous particles of small size and may be related to entities created in the early stages of combustion around the cylinder axis where fuel was available but soot was also oxidized in this high-temperature well-mixed zone. Only a small annular region [Fig. 6(*a*)], close to the bowl edge seems to correlate the presence of soot to oxygen depletion as observed in Fig. 7, where the iso-surface in the bowl embeds the volume where the mass fraction of oxygen is below 6%. The other characteristic population is along the wall and the top of the cylinder with reduced soot oxidation due to heat losses. Their different histories of soot creation dynamics, according to previous explanations, cause soot particles to survive in different regions in the cylinder at the end of the expansion with different implications in soot formation and oxidation, leading to different size distributions and hence the bimodal size distribution found in Fig. 5. However, it should be noted that this distribution is based on primary soot particle size and not on agglomerated clusters effectively gathered at an engine exhaust. The cluster size distribution, not predicted here, may have a different shape.

Conclusion

A soot formation model developed by Tesner et al., already acknowledged for its use in practical applications, has been extended through simple expressions based on kinetic theory. This more comprehensive model is now able to account for an important part of the soot formation history, to a certain level of approximation, which relies on the limiting step of the pyrolysis, the inception based on active radicals from the hydrocarbon breakdown and the growth of the primary particles through collision with each other and the fuel molecules in the surrounding gas. The system of equations is kept as simple as possible to save computational and tuning cost. The intermediate growth specie is bypassed for sake of simplicity, given the numerous approximations encountered at several levels in a real scale 3D simulation. The behavior of this model has been explored with respect to EGR and compared to the one-step model, commonly used by the engine design community. New insights into the soot population history in a diesel engine cylinder have been furthermore gained and active areas related to soot formation have been pointed out.

This modeling, compatible with engine design tools, reveals some important features of the primary particle history in two main zones in the cylinder, leading to two different populations of soot. Near the bowl edge, the remaining soot is explained by oxygen depletion while, close to the top and the wall, heat losses prevent the destruction of the soot so that much particles exist with a large size. The high-temperature and well mixed interior of the cylinder is populated by small soot particles so that two characteristic primary particle sizes may be encountered at the exhaust (this size distribution for the primary soot particles should not prevail of the fractal cluster size released at the exhaust). EGR leads to an increase in soot mass exhaust through an increase in both the number of primary particles and their diameter. The increase in the number of primary particles is related to presence of the fuel for a longer period of time and the increase in diameter may be linked to a weaker oxidation due to lower temperatures in the cylinder.

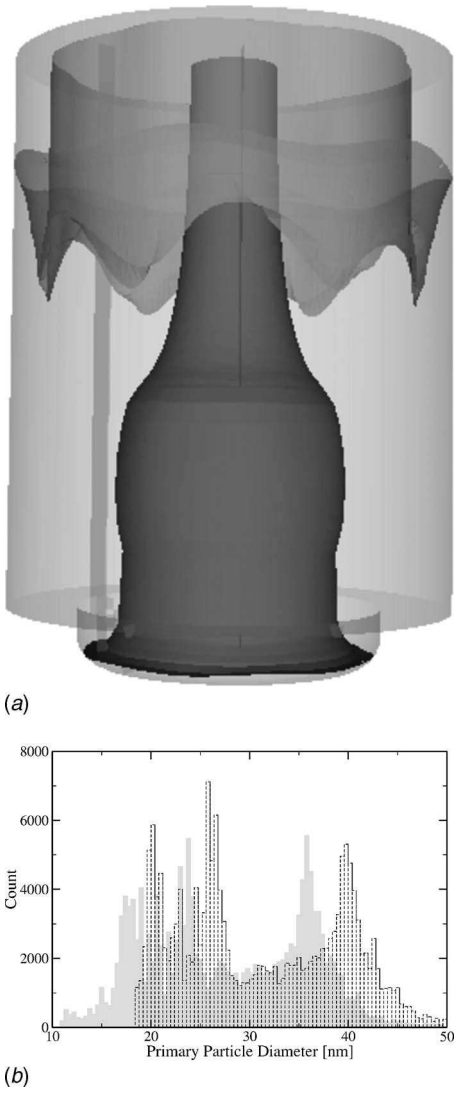

Fig. 5 (*a*) Picture EGR 0%. Plain iso-surface: Diameter below 20 nm. Transparent iso-surface: Diameter above 40 nm. (*b*) Particle diameter distribution at the exhaust (Grey: EGR 0%; Dashed: EGR 8%).

This soot model is of interest due to its ability to predict the primary particle size. However, the soot structure at the exhaust of an engine is an agglomeration of soot primary particles. Those structures appear following a fractal growth process which determines the final weight, size, and number of those clusters. Prediction of agglomeration might be an interesting future development for soot modeling dedicated to diesel engines design. In addition, further validation of the model with experimental data is warranted.

Acknowledgment

This research has been made possible by the funding received from the Government of Canada Program for Energy Research

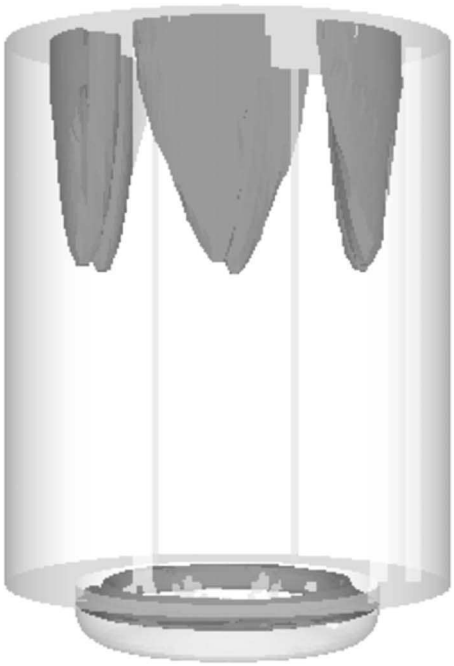

(*a*)

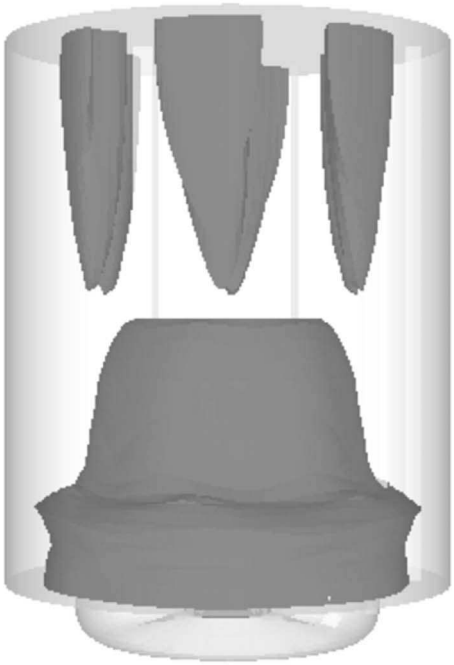

(*b*)

Fig. 6 Distribution of the two main soot zones at the end of the simulation. (*a*) Iso-surface (8.4×10^{-6}) of the soot mass fraction. (*b*) Iso-surface (1.6×10^{14} kg^{-1}) of the number of primary particles.

and Development (PERD/AFTER). The authors wish to thank Dr. S. C. Kong and Professor R. D. Reitz for providing the grid specification of the engine geometry and parameters.

Nomenclature

Only symbols that are either not available or different from those in the international nomenclature of thermal sciences are listed in the nomenclature.

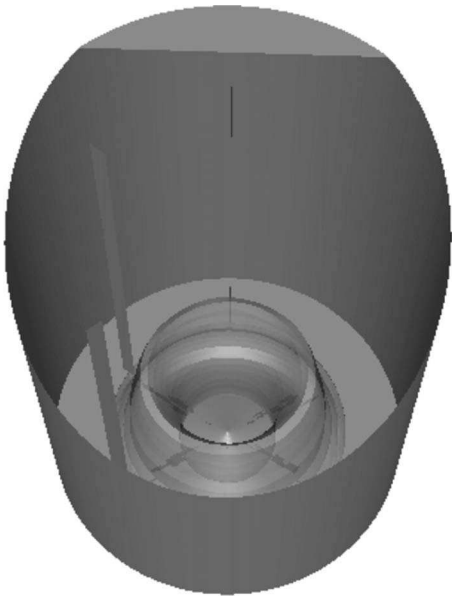

Fig. 7 Oxygen depletion in the bowl. The iso-surface draws a volume in which oxygen mass fraction is below 6%.

Capital Letters

A_s = primary particle surface (m^2)
D = primary particle diameter (nm)
F = branching-termination coefficient (s^{-1})
K_c = coagulation coefficient (m$^{5/2}$ K$^{-1/2}$ s^{-1})
$K_{G,\text{incep}}$ = growth coefficient (Kg m^3 s^{-1})
N = primary particle number density (m^{-3})
$T_{a_{n_o}}$ = fuel pyrolysis activation temperature (K)

Lowercase Letters

a = soot inception coefficient (s^{-1})
a_0 = preexponential constant of fuel pyrolysis (s^{-1})
b = termination coefficient (m^3/s)
g_0 = termination coefficient (m^3/s)
m_p = nominal mass of primary soot particles (kg)
n = radical number density (m^{-3})
n_o = radical production rate (s^{-1} m^{-3})

Subscripts

F = fuel species
i = cell number
o = inception
s = soot species

References

[1] Belardini, P., Bertoli, C., Ciajolo, A., D'Anna, A., and Del Giacomo, N., 1992, "Three Dimensional Calculations of D. I. Diesel Engine Combustion and Comparison With in Cylinder Sampling Valve Data," SAE Technical Paper No. 92225.
[2] U. S. E. P. A. (EPA), 2002, "Air Quality Criteria for Particulate Matter," Third external review draft EPA/600/P-99/002aC, Research Triangle Park, NC.
[3] 2001, "Réduire les émissions des Véhicules / Vehicle Emission Reductions," 92-82-11363-9, *Proceedings of the European Conference of Ministers of Transport (ECMT)*, OECD, Paris.
[4] Khan, G., and Greeves, A., 1974, *Method for Calculating the Formation and Combustion of Soot in Diesel Engines*, Scripta, Washington, DC, Chap. 25.
[5] Surovikin, V., 1976, "Analytical Description of the Processes of Nucleus-Formation and Growth of Particles of Carbon Black in the Thermal Decomposition of Aromatic Hydrocarbons in the Gas Phase," Solid Fuel Chem., **10**(1), pp. 92–101.
[6] Fusco, A., Knox-Kelecy, A., and Foster, D., 1994, "Application of a Phenomenological Soot Model to Diesel Engine Combustion," Proceedings of the International Symposium COMODIA 94, Yokohama, Japan.
[7] Appel, J., Bockhorn, H., and Frenklach, M., 2000, "Kinetic Modeling of Soot Formation With Detailed Chemistry and Physics: Laminar Premixed Flames of

C_2 Hydrocarbons," Combust. Flame, **121**(1/2), pp. 122–136.
[8] Tao, F., Golovitchev, V., and Chomiak, J., 2004, "A Phenomenological Model for the Prediction of Soot Formation in Diesel Spray Combustion," Combust. Flame, **136**(3), pp. 270–282.
[9] Ahmad, T., Plee, S., and Myers, J., 1985, "Computation of Nitric Oxide and Soot Emissions from Turbulent Diffusion Flames," J. Eng. Gas Turbines Power, **107**(1), pp. 48–53.
[10] Hiroyasu, H., and Nishida, K., 1989, "Simplified Three-Dimensional Modeling of Mixture Formation and Combustion in D. I. Diesel Engine," SAE Technical Paper No. 890269.
[11] Patterson, M., Kong, S., Hampson, G., and Reitz, R., 1994, "Modeling the Effects of Fuel Injection Characteristics on Diesel Engine Soot and NOx Emissions," SAE Technical Paper No. 940523.
[12] Han, Z., and Reitz, R., 1995, "Turbulence Modeling of Internal Combustion Engines using RNG κ-ε Models," Combust. Sci. Technol., **106**(4/6), pp. 267–295.
[13] Kong, S., Han, Z., and Reitz, R., 1995, "The Development and Application of a Diesel Ignition and Combustion Model for Multidimensional Engine Simulation," SAE Technical Paper No. 950278.
[14] Reitz, R., and Rutland, C., 1995, "Development and Testing of Diesel Engine CFD models," Prog. Energy Combust. Sci., **21**(2), pp. 173–196.
[15] Uludogan, A., Xin, J., and Reitz, R., 1996, "Exploring the Use of Multiple Injectors and Split Injection to Reduce D. I. Diesel Engine Emissions," SAE Technical Paper No. 962058.
[16] Han, Z., Uludogan, A., Hampson, G., and Reitz, R., 1996, "Mechanism of Soot and NOx Emission Reduction Using Multiple-Injection in a Diesel Engine," SAE Technical Paper No. 960633.
[17] Chan, M., Das, S., and Reitz, R., 1997, "Modeling Multiple Injection and EGR Effects on Diesel Engine Emissions," SAE Technical Paper No. 972864.
[18] Fuchs, T., and Rutland, C., 1998, "Intake Flow Effects on Combustion and Emissions in a Diesel Engine," SAE Technical Paper No. 980508.
[19] Das, S., Houtz, P., and Reitz, R., 1999, "Effect of Injection Spray Angle and Combustion Chamber Geometry on Engine Performance and Emission Characteristics of a Large Bore Diesel Engine," Proceedings of the Spring Technical Conference, ASME, Vol. 32–1, pp. 1–12.
[20] Jung, D., and Assanis, D., 2001, "Multi-Zone DI Diesel Spray Combustion Model for Cycle Simulation Studies of Engine Performance and Emissions," SAE Technical Paper No. 2001-01-1246.
[21] Tesner, P., Snegiriova, T., and Knorre, V., 1971, "Kinetics of Dispersed Carbon Formation," Combust. Flame, **17**(2), pp. 253–260.
[22] Mehler, R., Amann, M., and Schopp, W., 2002, "A Methodology to Estimate Changes in Statistical Life Expectancy Due to the Control of Particulate Matter Air Pollution," Technical Report No. IR-02-035, International Institute for Applied Systems Analysis, Laxenburg, Austria.
[23] Parker, J., 2005, "Air Pollution and Birth Weight among Term Infants in California," Pediatrics, **115**(1), pp. 121–128.
[24] Lee, J., Goto, Y., and Okada, M., 2002, "Measurement of the Diesel Exhaust Particle Reduction Effect and Particle Size Distribution in a Transient Cycle Mode With an Installed Diesel Particulate Filter (DPF)," SAE Technical Paper No. 2002-01-1005.
[25] Moss, J., Stewart, C., and Young, K., 1995, "Modeling Soot Formation and Burnout in a High Temperature Laminar Diffusion Flame Burning under Oxygen-Enriched Conditions," Combust. Flame, **101**(4), pp. 491–500.
[26] Leung, K., Lindstedt, R., and Jones, W., 1991, "A Simplified Reaction Mechanism for Soot Formation in Nonpremixed Flames," Combust. Flame, **87**(3/4), pp. 289–305.
[27] Bédat, B., Egolfopoulos, F. N., and Poinsot, T., 1999, "Direct Numerical Simulation of Heat Release and NO_x Formation in Turbulent Nonpremixed Flames," Combust. Flame, **119**(1/2), pp. 69–83.
[28] Nagle, J., and Strickland-Constable, R., 1962, "Oxidation of Carbon Between 1000–2000°C," *Proceedings of the Fifth Conference on Carbon*, Pergamon, London, pp. 154–164.
[29] Fenimore, C., and Jones, G., 1967, "Oxidation of Soot by Hydroxyl Radicals," J. Phys. Chem., **71**(3), pp. 593–597.
[30] Bradley, D., Dixon-Lewis, G., El-Din Habik, S., and Mushi, E., 1984, "The Oxidation of Graphite Powder in Flame Reaction Zones," *Proceedings of the 20th International Symposium on Combustion*, The Combustion Institute, Pittsburgh, pp. 931–940.
[31] Garo, A., 2004, private communication.
[32] Westbrook, C., and Dryer, F., 1984, "Chemical Kinetic Modelling of Hydrocarbon Combustion," Prog. Energy Combust. Sci., **10**(1), pp. 1–57.
[33] Magnussen, B., and Hjertager, B., 1976, "On Mathematical Modeling of Turbulent Combustion With Special Emphasis on Soot Formation and Combustion," *Proceedings of the 16th International Symposium on Combustion*, The Combustion Institute, Pittsburgh, pp. 719–729.
[34] Methodology volume, Star-CD, 2004, Edition.
[35] Huh, K., and Gosman, A., 1991, "A Phenomenological Model of Diesel Spray Atomisation," Proceedings of the International Conference on Multiphase Flows (ICMF'91), Tsukuba, Japan.
[36] Reitz, R., and Diwakar, R., 1986, "Effect of Drop Breakup on Fuel Sprays," SAE Technical Paper No. 860469.
[37] Mastorakos, E., and Wright, Y. M., 2003, "Simulations of Turbulent Spray Auto-Ignition With Elliptic Conditional Moment Closure," Proceedings of the European Combustion Meeting, Orléans, France.
[38] Yakhot, V., Orszag, S., Thangam, S., Gatski, T., and Speziale, C., 1992, "Development of Turbulence Models for Shear Flows by a Double Expansion Technique," Phys. Fluids A, **4**(7), pp. 1510–1520.
[39] Launder, B., and Spalding, D., 1974, "The Numerical Computation of Turbulent Flows," Comput. Methods Appl. Mech. Eng., **3**(2), pp. 269–289.
[40] Jayatilleka, C., 1969, "The Influence of Prandtl Number and Surface Roughness on the Resistance of the Laminar Sub-Layer to Momentum and Heat Transfer," Prog. Heat Mass Transfer, **1**, pp. 193–330.
[41] McLandress, A., Emerson, R., McDowell, P., and Rutland, C., 1996, "Intake and in-Cylinder Flow Modeling Characterization of Mixing and Comparison With Flow Bench Results," SAE Technical Paper No. 960635.
[42] Neill, W. S., and Chippior, W., 2002, NRC Report No. PET-1528-02S.
[43] Hergart, C., Barths, H., and Peters, N., 2000, "Using Representative Interactive Flamelets in Three-Dimensional Modelling of the Diesel Combustion Process Including Effects of Heat Transfer," Proceedings of the International Multidimensional Engine Modeling User's Group Meeting, Madison, WI.
[44] Hergart, C., and Peters, N., 2002, "Applying the Representative Interactive Flamelet Model to Evaluate the Potential Effect of Wall Heat Transfer on Soot Emissions in a Small-Bore Direct-Injection Diesel Engine," J. Eng. Gas Turbines Power, **124**(4), pp. 1042–1052.
[45] Tao, F., Srinivas, S., Reitz, R. D., and Foster, D. E., 2004, "Current Status of Soot Modeling Applied to Diesel Combustion Simulations," Proceedings of the International Symposium COMODIA 2004, Yokohama, Japan.
[46] Khan, I. M., Wang, C. H. T., and Langridge, B. E., 1971, "Coagulation and Combustion of Soot Particles in Diesel Engines," Combust. Flame, **17**(3), pp. 408–419.
[47] Smith, O. I., 1981, "Fundamentals of Soot Formation in Flames With Application to Diesel Engine Particulate Emissions," Prog. Energy Combust. Sci., **7**(4), pp. 275–291.